Iterative Detection of Multicode DS-CDMA Signals with Strong Nonlinear Distortion Effects

Rui Dinis, *Member, IEEE* and Paulo Silva

***Abstract*—Whenever a direct sequence code division multiple access (DS-CDMA) signal is the sum of several components associated to different spreading codes (e.g., the DS-CDMA signal to be transmitted by the base station (BS) in the downlink or any multicode DS-CDMA signal) it has high envelope fluctuations and a high peak-to-mean envelope power ratio (PMEPR) setting strong linearity requirements for the power amplifiers. For this reason, it is desirable to reduce the envelope fluctuations of the transmitted signals.**

The use of clipping techniques combined with frequency-domain filtering was shown to be an effective way of reducing the envelope fluctuations (and, inherently, the PMEPR) of DS-CDMA signals, while maintaining the spectral occupation of the corresponding conventional DS-CDMA signals. To avoid PMEPR regrowth effects the clipping and filtering operations can be repeated several times. However, the performance degradation due to nonlinear distortion effects on the transmitted signals can be relatively high, especially when a very low PMEPR is intended (e.g., when a low clipping level and several iterations are adopted). This can be especially serious if different powers are assigned to different spreading codes.

To avoid significant performance degradation in these situations, we consider an improved receiver where there is an iterative estimation and cancelation of nonlinear distortion effects. Our performance results show that the proposed receiver allows significant performance improvements after just a few iterations, even when we have strong nonlinear distortion effects.

***Index Terms*—DS-CDMA, envelope fluctuations, iterative detection, nonlinear distortion, signal processing.**

I. Introduction

Direct Sequence Code Division Multiple Access (DS-CDMA) schemes have been selected for several wireless systems, namely due to their good capacities and performances in time-dispersive channels [1], [2]. These techniques are good candidates for broadband wireless systems, especially when combined with cyclic prefix (CP) assisted block transmission techniques and frequency-domain equalization (FDE) schemes [3], [4].

However, envelope fluctuations and peak-to-mean envelope power ratio (PMEPR) of DS-CDMA signals can be very high when we combine a large number of signals with different spreading codes, namely at the downlink transmission and/or for multicode CDMA schemes [5], leading to amplification difficulties. For this reason, several techniques were proposed for designing low-PMEPR DS-CDMA signals, e.g., by adding unused codes [6] or through suitable signal processing techniques [7]-[9].

A simple and promising method for reducing the PMEPR of DS-CDMA signals it to employ a nonlinear clipping operation in the time-domain followed by a linear, frequency-domain filtering operation so as to generate a low-PMEPR version of the DS-CDMA signal, occupying the same bandwidth of the corresponding conventional DS-CDMA signal [8], [9] (similar techniques have also been proposed for reducing the envelope fluctuations of orthogonal frequency division multiplexing (OFDM) signals [10]). However, the filtering operation produces some envelope fluctuations regrowth, limiting the achievable PMEPR [9]. As with OFDM schemes [11], [12], by repeating the clipping and filtering procedures we can reduce the PMEPR regrowth in multicode DS-CDMA schemes [13]. However, nonlinear distortion levels increase when we repeat the clipping and filtering procedures, leading to performance degradation. This performance degradation can be particularly high when we have different powers assigned to different spreading codes, especially for the spreading codes with lower power [14]. A scenario where this effect might be significant is for multi-resolution broadcasting systems [15], [16], where we transmit simultaneously several parallel data streams with different powers so as to have different error protections. For DS-CDMA systems, this can be achieved by assigning to each resolution a subset of the available spreading codes and a different power to each subset (i.e., the spreading codes with higher power have higher error protection and, therefore, are associated to the basic (lower) resolution).

We can improve significantly the performance of nonlinearly-distorted OFDM schemes by employing enhanced receivers with iterative estimation and cancelation of nonlinear distortion effects [17], [18]. This concept was extended to multicode DS-CDMA systems in [14]. To cope with time-dispersive channels, a linear frequency-domain equalizer (FDE) was employed before the iterative estimation and cancelation of nonlinear distortion effects. However, error propagation effects preclude an efficient estimation and cancelation of nonlinear distortion effects when in the presence of severe nonlinear distortion and/or at moderate and low signal-to-noise ratios (SNR). In fact, for those conditions the performance with iterative estimation and cancelation of nonlinear effects can be worse than without compensation [18]. When suitable channel coding schemes are employed the working region usually corresponds to low or moderate SNR values, which reduces the interest of those techniques

Rui Dinis is with the Instituto de Telecomunicações, Lisbon, Portugal, and also with the Faculdade de Ciências e Tecnologia, Universidade Nova de Lisboa, Portugal (e-mail: rdinis@fct.unl.pt).

Paulo Silva is with the Instituto de Telecomunicações, Lisbon, Portugal, and also with Instituto Superior de Engenharia, Universidade do Algarve, 8005-139 Faro, Portugal (e-mail: psilva@ualg.pt).

This work was supported in part by Fundação para a Ciência e Tecnologia (pluriannual funding, U-BOAT project PTDC/EEA-TEL/67066/2006 and the FCT/POCI 2010 research grant SFRH/BD/24520/2005).

for the estimation and cancelation of nonlinear distortion effects.

Usually the FDE is optimized under the minimum mean-squared error (MMSE) criterium to avoid noise enhancement effects inherent to a zero forcing-based (ZF) optimization, especially when we have deep in-band notches [19]. This means that the spreading codes are not perfectly orthogonalized by a linear FDE, which might lead to severe interference levels especially when different powers are assigned to different spreading codes. It is well-known that nonlinear equalizers can significantly outperform linear equalizers. A promising iterative block decision feedback equalization (IB-DFE) approach was proposed for CP-assisted single carrier (SC) schemes [20], which can be regarded as a DFE where both the feedforward and the feedback parts are implemented in the frequency-domain. This concept was extended to scenarios with space diversity [21] and to layered space-time systems [22], [23]. These schemes were also shown to be very efficient for the downlink of CP-assisted CDMA systems [24], [25].

In this paper we consider multi-resolution broadcasting systems using CP-assisted DS-CDMA schemes. We have several parallel streams with different powers so as to achieve multi-resolution. The transmitted signals have very low PMEPR thanks to the adoption of clipping (with low clipping level) and filtering techniques, which are repeated several times. We modify the approach of [14] so as to cope with its major limitations, namely: the use of a linear FDE; the separate implementation of the FDE part and estimation and compensation of nonlinear distortion effects; error propagation effects in the estimation and compensation of nonlinear distortion; poor performance in the presence of severely nonlinear distortion effects and/or at low-to-moderate SNRs. We consider an iterative frequency-domain receiver where the FDE operation and the estimation and cancelation of nonlinear distortion effects are jointly performed in an iterative way. Therefore, our receiver can be regarded as an IB-DFE receiver with estimation and cancelation of nonlinear distortion effects for each iteration. To improve the performance at low-to-moderate SNR we consider a turbo receiver combined with a threshold-based cancelation of nonlinear distortion effects. We also consider a turbo variant of our receiver where the channel decoding is performed for each iteration. We include the statistical characterization of the transmitted signals, which can be regarded as the extension of the approach of [9] to the case where the clipping and filtering operations are repeated several times. This characterization is then used for obtaining the receiver parameters.

The paper is organized as follows: In Sec. II, we describe the transmitter structure. Sec. III presents a statistical characterization of the transmitted signals which is used for performance evaluation purposes in Sec. IV. Sec. V-A to C describe the receiver structure proposed in this paper and Sec. V-D discuses some implementation issues. A set of performance results is presented in Sec. VI and Sec. VII is concerned with the conclusions of this paper.

II. Transmitter Structure

In this paper we consider the downlink transmission in DS-CDMA systems employing CP-assisted block transmission techniques combined with FDE schemes. The base station (BS) simultaneously transmits data blocks for N_R resolutions. For the sake of simplicity, we assume an orthogonal spreading with K_r spreading codes associated to the rth resolution and the same spreading factor K for all spreading codes. This means that

$$\sum_{r=1}^{N_R} K_r \leq K. \tag{1}$$

We have a separate channel coding chain for each resolution (channel encoder, interleaver, etc.) as shown in Fig. 1(a). The coded bits associated to the rth resolution are interleaved and mapped in the symbols $\{a_{m,r'}; r' \in \Psi_r\}$, with Ψ_r denoting a set with the indexes r' of the spreading codes associated to the rth resolution (naturally, it is assumed that $\Psi_{r_1} \cap \Psi_{r_2} = \emptyset$ for $r_1 \neq r_2$, i.e., different spreading codes are assigned to different resolutions). For the sake of simplicity, we assume that all K orthogonal spreading codes are used[1] (the extension to other cases is straightforward), which means that

$$\bigcup_{r=1}^{N_R} \Psi_r = \{0, 1, \ldots, K-1\}. \tag{2}$$

The block of chips to be transmitted by the BS is $\{s_n; n = 0, 1, \ldots, N-1\}$, where the "overall" chip symbol, s_n, is given by

$$s_n = \sum_{r=1}^{N_R} \sum_{r' \in \Psi_r} \xi_r s_{n,r'}, \tag{3}$$

with

$$s_{n,r'} = c_{n,r'} a_{\lfloor n/K \rfloor, r'} \tag{4}$$

denoting the nth chip for the r'th spreading code ($\lfloor x \rfloor$ denotes 'larger integer not higher that x'), where $\{c_{n,r'}; n = 0, 1, \ldots, N-1\}$ is the corresponding spreading sequence and $\{a_{m,r'}; m = 0, 1, \ldots, N/K-1\}$ is the block of symbols associated to the r'th spreading code. The power assigned to the rth resolution is proportional to $|\xi_r|^2$.

To reduce the PMEPR of the transmitted signals we consider the transmitter structure proposed in [26] and depicted in Fig. 1(b). The block of modified samples $\{s_n^{Tx}; n = 0, 1, \ldots, N-1\}$ is formed from the original block of samples $\{s_n; n = 0, 1, \ldots, N-1\}$ in the following way: The original block of samples is passed to the frequency-domain by a N-point discrete Fourier transform (DFT), leading to the block $\{S_k; k = 0, 1, \ldots, N-1\}$. Then $N'-N$ zeros are added to the block $\{S_k; k = 0, 1 \ldots, N-1\}$ so as to form the augmented block $\{S'_k; k = 0, 1 \ldots, N'-1\}$, with

$$S'_k = \begin{cases} S_k, & 0 \leq k < \frac{N}{2} - 1 \\ S_{k-N'}, & N' - \frac{N}{2} \leq k < N' - 1 \\ 0, & \text{otherwise.} \end{cases} . \tag{5}$$

An inverse discrete Fourier transform (IDFT) brings the augmented block $\{S'_k; k = 0, 1 \ldots, N'-1\}$ back to the

[1] This means that we have an equality in (1).

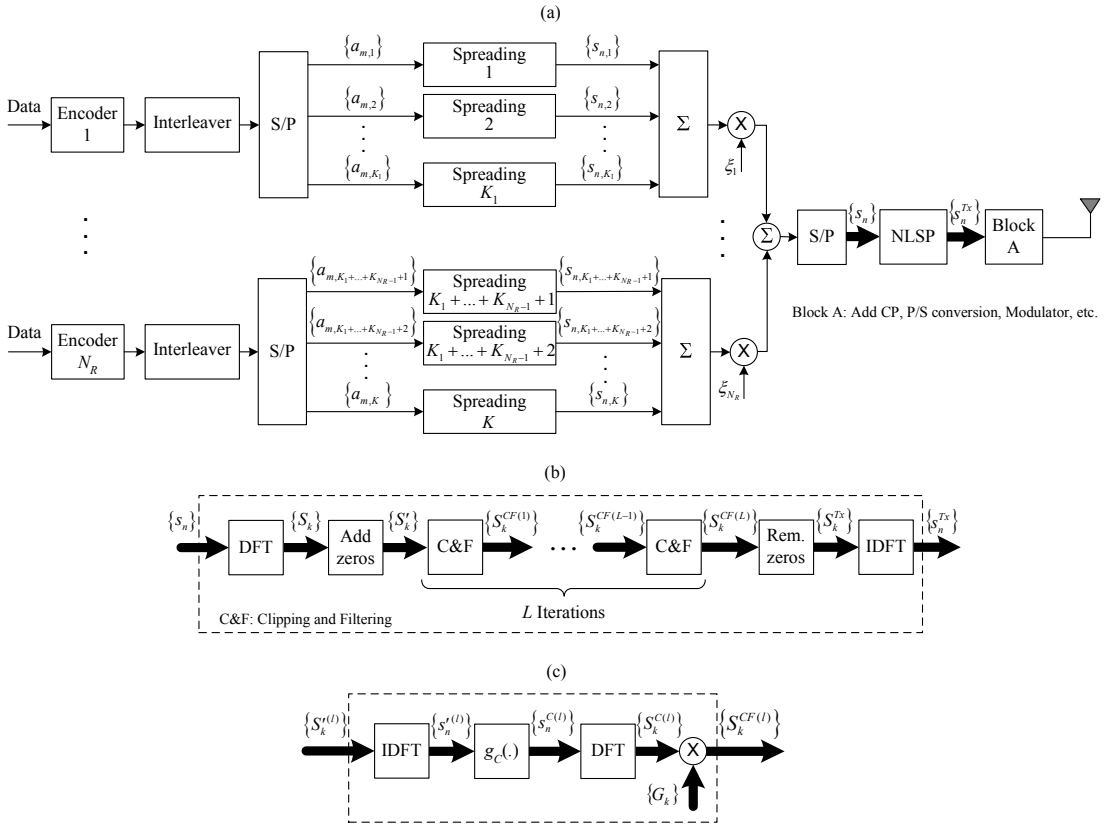

Fig. 1. Transmitter structure considered in this paper (a), detail of the nonlinear signal processing (NLSP) block (b) and clipping and filtering (C&F) block (c).

time-domain (see Fig. 1(c)), resulting the block $\{s'_n; n = 0, 1, \ldots, N'-1\}$. These time-domain samples, which can be regarded as a sampled version of the DS-CDMA block, with the oversampling factor[2] $M_{Tx} = N'/N$, are submitted to a nonlinear operation so as to reduce the corresponding PMEPR, leading to the modified samples

$$s_n^C = g_C(|s'_n|) \exp\left(j \arg(s'_n)\right). \tag{6}$$

A possible nonlinear characteristic is an ideal envelope clipping with clipping level s_M, i.e.,

$$g_C(|s'_n|) = \begin{cases} |s'_n|, & |s'_n| < s_M \\ s_M, & |s'_n| \geq s_M \end{cases}. \tag{7}$$

A DFT brings the nonlinearly modified samples back to the frequency-domain, leading to the block $\{S_k^C; k = 0, 1, \ldots, N'-1\}$, where a shaping operation corresponding to a frequency-domain filtering is performed so as to obtain the block $\{S_k^{CF} = S_k^C G_k; k = 0, 1, \ldots, N'-1\}$, with

$$G_k = \begin{cases} 1, & 0 \leq k < \frac{N}{2} - 1,\ N' - \frac{N}{2} \leq k < N' - 1 \\ 0, & \text{otherwise} \end{cases}. \tag{8}$$

To reduce the PMEPR regrowth associated to the filtering operation, the signal processing operations which lead from $\{S'_k; k = 0, 1 \ldots, N'-1\}$ to $\{S_k^{CF}; k = 0, 1 \ldots, N'-1\}$ in Fig. 1(c) are repeated, in an iterative way, L times:

$$S_k'^{(l)} = \begin{cases} S'_k, & l = 1 \\ S_k^{CF(l-1)}, & l > 1 \end{cases}, \tag{9}$$

where each superscript l concerns a given iteration. From the block $\{S_k^{CF(L)}; k = 0, 1, \ldots, N'-1\}$ we form the "final" frequency-domain block $\{S_k^{Tx}; k = 0, 1, \ldots, N-1\}$ by removing $N'-N$ zero-valued frequency-domain samples, i.e.,

$$S_k^{Tx} = \begin{cases} S_k^{CF(L)}, & 0 \leq k \leq \frac{N}{2} - 1 \\ S_{N'-N+k}^{CF(L)}, & \frac{N}{2} \leq k \leq N-1 \end{cases}. \tag{10}$$

Finally, the corresponding IDFT is computed, leading to the block of modified samples $\{s_n^{Tx}; n = 0, 1, \ldots, N-1\}$. The rest of the transmitter is similar to a conventional, CP-assisted DS-CDMA transmitter (CP insertion, D/A conversion, etc.).

For a given size-N input block with duration T, a specific signal processing scheme can be designed through the selection of $M_{Tx} = N'/N$, the nonlinear device and the number of clipping and filtering iterations. The block $\{s'_n; n = 0, 1, \ldots, N'-1\}$ can be regarded as a sampled version of

$$s(t) = \sum_{n=-\infty}^{+\infty} s'_n h_T\left(t - n\frac{T}{N'}\right), \tag{11}$$

with the oversampling factor M_{Tx}, provided that the roll-off factor of the reconstruction filter $h_T(t)$ is small. Clearly, the PMEPR of the transmitted signal depends on the adopted pulse

[2]As shown in [9], $M_{Tx} > 1$ reduces the "in-band self-interference" effects of the nonlinearity, while increasing the "out-of-band self-interference" levels. The oversampling is also required for an effective PMEPR reduction since the envelope excursions of the samples are only similar to the excursions of the corresponding analog signal for an oversampling factor of, at least, 2 or 4.

shape $h_T(t)$. For a square-root raised cosine pulse there is a slight increase in the PMEPR with the roll-off factor (less then 1 dB [9]).

The nonlinear operation can be selected so as to ensure a PMEPR reduction and the subsequent frequency-domain operation using the set $\{G_k; k = 0, 1 \ldots, N' - 1\}$ provides a complementary filtering effect, eliminating the out-of-band distortion effects of the nonlinearity. However, this filtering operation produces some regrowth on the envelope fluctuations. By repeatedly using, in an iterative way, the nonlinear operation and the subsequent frequency-domain filtering, we can achieve lower envelope fluctuations while preserving a low out-of-band radiation level. For instance, Fig. 2 shows the histogram of $|s_n^{CF}|$ after 1, 2, 3 and 4 clipping and filtering operations for normalized clipping levels of $s_M/\sigma = 0.5$, 1.0 and 2.0, where $\sigma^2 = E\left[|s'_n|^2\right]/2$, as well as the histogram of $|s'_n|$.

III. Statistical Characterization of the Transmitted Signals

In this section we present a statistical characterization of the modified time-domain samples $\{s_n^{Tx}; n = 0, 1, \ldots, N-1\}$ that replace the block of time-domain samples of conventional DS-CDMA, $\{s_n; n = 0, 1, \ldots, N-1\}$. This characterization is accurate whenever the number of spreading codes is high enough (say, several tens of spreading codes) to allow a Gaussian approximation of conventional DS-CDMA signals [to validate the Gaussian approximation the power associated to a given spreading code cannot be a significant fraction of the total power (see Fig. 3, where $N = K = 256$)[3]]. This statistical characterization can then be used for performance evaluation purposes, as described in the following section.

A. Basic Signal Processing Scheme

Let us assume that the signal at the input of the memoryless nonlinear device has a Gaussian nature. In that case, it is well-known that the signal at the nonlinearity output can be decomposed into uncorrelated "useful" and "self-interference" components [27]:

$$s_n^C = \alpha s'_n + d_n \tag{12}$$

where $E[s'_n d^*_{n'}] = 0$ and $\alpha = E[|s'_n|\ g_C(|s'_n|)]/E[|s'_n|^2]$. Clearly, the average power of the useful component at the nonlinearity output is $P_{NL}^S = |\alpha^2|\sigma^2$, and the average power of the self-interference component is $P_{NL}^I = P_{NL} - P_{NL}^S$, where $P_{NL} = E[g_C^2(|s'_n|)]/2$ denotes the average power of the signal at the nonlinearity output.

It can be shown that the autocorrelation of the output samples $R_s^C(n-n') = E[s_n^C s_{n'}^{C*}]$ can be expressed as a function of the autocorrelation of the input samples $R_s(n-n') = E[s'_n s'^*_{n'}]$ as follows [9]:

$$\begin{aligned} & E[s_n^C s_{n'}^{C*}] = R_s^C(n-n') \\ = & \sum_{\gamma=0}^{+\infty} 2P_{2\gamma+1} \frac{[R_s(n-n')]^{\gamma+1}\,[R_s^*(n-n')]^{\gamma}}{[R_s(0)]^{2\gamma+1}}, \end{aligned} \tag{13}$$

[3]It should be pointed out that for the multi-resolution scheme considered in this paper we need to have several spreading codes associated to each resolution to validate a Gaussian approximation for s_n (i.e., we need to have $K_r >> 1$, especially for the spreading codes with higher assigned power).

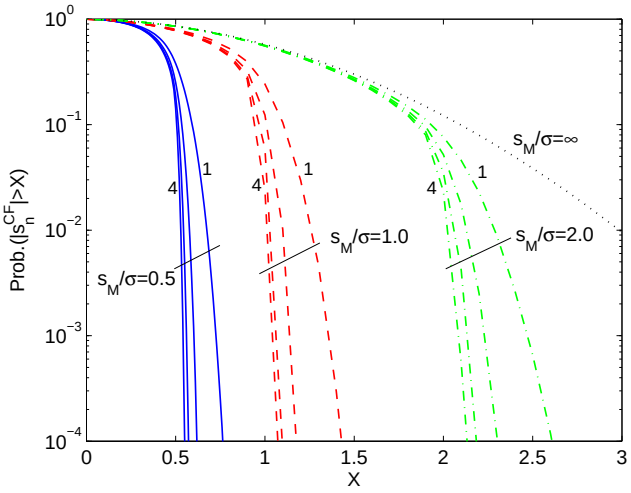

Fig. 2. Histogram of $|s_n^{CF}|$ after 1, 2, 3 and 4 clipping and filtering operations for normalized clipping levels of $s_M/\sigma = 0.5$, 1.0 and 2.0, as well as the histogram of $|s'_n|$ (doted line).

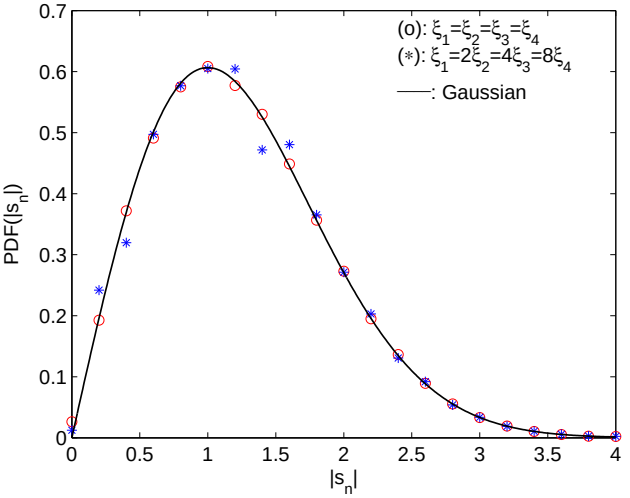

Fig. 3. Histogram of $|s_n|$ when $N = K = 256$.

where the coefficient $P_{2\gamma+1}$ denotes the total power associated to the inter-modulation product (IMP) of order $2\gamma+1$, which can be calculated as described in [9], following [28], [29]. If $E[s_n s^*_{n'}] = 2\sigma_s^2 \delta_{n,n'}$ (where $\delta_{n,n'} = 1$ if $n = n'$ and 0 otherwise) then $E[S_k S^*_{k'}] = 2N\sigma_s^2 \delta_{n,n'}$ and

$$\begin{aligned} & E\left[s'_n s'^*_{n'}\right] = R_s(n-n') \\ = & \ 2\sigma^2 \frac{\operatorname{sinc}\left[\frac{N(n-n')}{N'}\right]}{\operatorname{sinc}\left(\frac{n-n'}{N'}\right)} \exp\left[-\frac{j\pi(n-n')}{N'}\right], \end{aligned} \tag{14}$$

$(n, n' = 0, 1, \ldots, N'-1)$, with

$$\sigma^2 = \frac{N^2}{(N')^2}\sigma_s^2 = \frac{\sigma_s^2}{M_{Tx}^2}. \tag{15}$$

Since $R_s^C(n-n') = |\alpha|^2 R_s(n-n') + R_d(n-n')$, where $R_d(n-n') = E[d_n d^*_{n'}]$, it can be easily recognized that $P_1 = P_{NL}^S = |\alpha|^2\sigma^2$ and $R_d(n-n')$ is obtained by using $\sum_{\gamma=1}^{\infty}$ instead of $\sum_{\gamma=0}^{\infty}$ in the right-hand side of (13).

Having in mind (12) and the signal processing chain in Fig. 1(c), the frequency-domain block $\{S_k^{CF} = S_k^C G_k; k = 0, 1, \ldots, N'-1\}$ can obviously be decomposed into useful and self-interference components: $S_k^{CF} = \alpha S'_k G_k + D_k G_k$, where $\{D_k; k = 0, 1, \ldots, N'-1\}$ denotes the DFT of $\{d_n; n = 0, 1, \ldots, N'-1\}$.

It can be shown that $E[D_k] = 0$ and $E[D_k D_{k'}^*] = N' G_d(k)\delta_{k,k'}$ $(k, k' = 0, 1, \ldots, N'-1)$, where $\{G_d(k); k = 0, 1, \ldots, N'-1\}$ is the DFT of $\{R_d(n); n = 0, 1, \ldots, N'-1\}$. Similarly, $E[S_k^C S_{k'}^{C*}] = N' G_s^C(k)\delta_{k,k'}$ where $\{G_s^C(k) = |\alpha|^2 G_s(k) + G_d(k); k = 0, 1, \ldots, N'-1\}$ is the DFT of $\{R_s^C(n); k = 0, 1, \ldots, N'-1\}$, with $R_s^C(n)$ given by (13), and $\{G_s(k); k = 0, 1, \ldots, N'-1\}$ the DFT of $\{R_s(n); n = 0, 1, \ldots, N'-1\}$. Therefore,

$$E\left[S_k^{CF} S_{k'}^{CF*}\right] = G_k G_{k'}^* E\left[S_k^C S_{k'}^{C*}\right] = \begin{cases} N'|G_k|^2 G_s^C(k), & k = k' \\ 0, & k \neq k' \end{cases} . \quad (16)$$

The "final" frequency-domain block can also be decomposed into uncorrelated useful and self-interference terms, $S_k^{Tx} = \alpha S_k + D_k^{Tx}$, with

$$D_k^{Tx} = \begin{cases} D_k, & 0 \leq k \leq \frac{N}{2} - 1 \\ D_{N'-N+k}, & \frac{N}{2} \leq k \leq N-1 \end{cases} . \quad (17)$$

This means that

$$s_n^{Tx} = \alpha s_n + d_n^{Tx}, \quad (18)$$

where $\{d_n^{Tx}; n = 0, 1, \ldots, N-1\}$ is the IDFT of $\{D_k^{Tx}; k = 0, 1, \ldots, N-1\}$.

B. Iterative Signal Processing Scheme

For the iterative signal processing scheme in Fig. 1(b) the Gaussian approximation for the samples at the input to the nonlinearity is no longer valid after the first iteration. Therefore, the method for modeling the transmitted blocks needs to be modified. Our simulations have shown that

$$S_k^{CF(l)} \approx \alpha_k^{(l)} S'_k G_k + D_k^{(l)} G_k, \quad (19)$$

with $\alpha_k^{(l)}$ depending on k when $l > 1$, as shown in Fig. 4(a). This means that the kth component of the frequency-domain block, for the lth iteration, can still be decomposed as a sum of two uncorrelated components (a similar behavior was observed in [12]). The statistical characterization concerning the first iteration, described above, can be regarded as a special case of (19) with constant $\alpha_k^{(1)}$; in this case, the values of $\alpha_k^{(1)}$ and $E[|D_k^{(1)}|^2]$ can be obtained analytically as described in the previous subsection. For the remaining iterations ($l > 1$) the values of $\alpha_k^{(l)}$ and $E[|D_k^{(l)}|^2]$ can be obtained by simulation in the following way:

$$\alpha_k^{(l)} = \frac{E\left[S_k^{C(l)} S_k'^*\right]}{E\left[|S'_k|^2\right]} \quad (20)$$

and

$$E\left[|D_k^{(l)}|^2\right] = E\left[|S_k^{C(l)} - \alpha_k^{(l)} S'_k|^2\right], \quad (21)$$

respectively. Fig. 4 shows the values of $\alpha_k^{(l)}$ and $E[|D_k^{(l)}|^2]$ after 1, 2, 4 and 8 iterations for a normalized clipping level of $s_M/\sigma = 0.5$. Our simulations also indicate that $E\left[D_k^{(l)}\right] = 0$ and $E\left[D_k^{(l)} D_{k'}^{(l)*}\right] \approx 0, k \neq k'$, as with the basic transmitter structure (i.e., with a single clipping and filtering procedure).

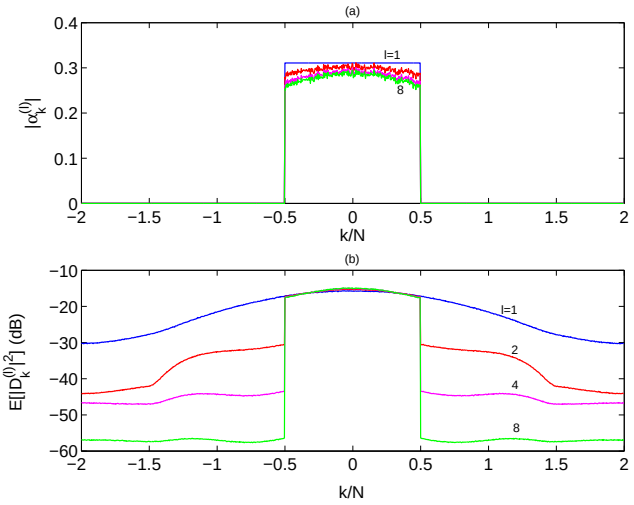

Fig. 4. Evolution of $|\alpha_k^{(l)}|$ (a) and power spectral density (PSD) of the interference component, $E[|D_k^{(l)}|^2]$ (b), after 1, 2, 4 and 8 C&F operations with a normalized clipping level of $s_M/\sigma = 0.5$.

From (10) and (19), it is clear that the samples $\{S_k^{Tx}; k = 0, 1, ..., N-1\}$ can be decomposed into uncorrelated "useful" and "self-interference" terms:

$$S_k^{Tx} = \alpha_k^{Tx} S_k + D_k^{Tx}, \quad (22)$$

with

$$\alpha_k^{Tx} = \begin{cases} \alpha_k^{(L)}, & 0 \leq k \leq \frac{N}{2} - 1 \\ \alpha_{N'-N+k}^{(L)}, & \frac{N}{2} \leq k \leq N-1 \end{cases} \quad (23)$$

and $\{D_k^{Tx}; k = 0, 1, ..., N-1\}$ related to $\{D_k^{(L)}; k = 0, 1, ..., N'-1\}$ as in (17). This means that $s_n^{Tx} = s_n^U + d_n^{Tx}$, where $\{s_n^U; n = 0, 1, \ldots, N-1\}$ is the IDFT of $\{\alpha_k^{Tx} S_k; k = 0, 1, \ldots, N-1\}$ (corresponding to the "useful" component of the transmitted signal) and $\{d_n^{Tx}; n = 0, 1, \ldots, N-1\}$ is the IDFT of $\{D_k^{Tx}; k = 0, 1, \ldots, N-1\}$ (corresponding to the "self-interference" component on the transmitted signal). Therefore, the modified samples $\{s_n^{Tx}; n = 0, 1, \ldots, N-1\}$ can always be decomposed into uncorrelated "useful" and "self-interference" components regardless of the number of clipping and filtering procedures. However, after the first iteration, the "useful" component is no longer proportional to the original samples, $\{s_n; n = 0, 1, ..., N-1\}$, due to the filtering effect inherent to α_k^{Tx} (see Fig. 4(a)).

IV. Performance Evaluation

Since $E[D_k^{(l)} D_{k'}^{(l)*}] \approx 0$, $k \neq k'$, we have $E[S_k^{CF(l)} S_{k'}^{CF(l)*}] \approx 0, k \neq k'$, leading to $E[S_k^{Tx} S_{k'}^{Tx*}] = 0$ for $k \neq k'$. Consequently, it can be shown that the power spectral density (PSD) of the transmitted signals is [9]

$$G_{Tx}(f) = \frac{|H_T(f)|^2}{T^3} \sum_{k=-\infty}^{+\infty} E\left[|S_k^{Tx}|^2\right] \left| X\left(f - \frac{k}{T}\right)\right|^2, \quad (24)$$

TABLE I
VALUES OF η_S, PMEPR AND SIR FOR THE TRANSMITTED SIGNALS.

s_M/σ	η_S (dB)				PMEPR (dB)				SIR (dB)			
	Iterations				Iterations				Iterations			
	1	2	4	8	1	2	4	8	1	2	4	8
0.5	-0.54	-0.64	-0.71	-0.74	4.1	3.0	2.0	1.7	8.8	7.9	7.5	7.3
1.0	-0.32	-0.42	-0.48	-0.50	4.4	3.4	2.4	2.1	11.1	10.0	9.3	9.1
1.5	-0.15	-0.21	-0.25	-0.27	5.0	4.0	3.2	2.9	14.6	13.0	12.2	12.0
2.0	-0.05	-0.08	-0.10	-0.11	5.7	4.9	4.2	4.0	19.4	17.4	16.3	15.9

with the block duration $T = NT_c$, where T_c is the chip duration, $H_T(f)$ the frequency response of the reconstruction filter and $X(f) = T\text{sinc}(fT)$ (it is assumed that $S_k^{Tx} = S_{k+N}^{Tx}, \forall_k$, i.e., S_k^{Tx} is periodic, with period N). This means that the spectral occupations of the modified signal and the corresponding conventional DS-CDMA signal are similar when G_k follows (8) regardless of the clipping level and the number of iterations.

Clearly, the performance of the proposed transmitter structure is worse than the performance of a conventional DS-CDMA transmitter. The performance degradation results from the fact that just a fraction

$$\eta_S = \frac{\sum_{n=0}^{N-1} E\left[|s_n^U|^2\right]}{\sum_{n=0}^{N-1} E\left[|s_n^U|^2\right] + \sum_{n=0}^{N-1} E\left[|d_n^{Tx}|^2\right]} \tag{25}$$

of the total transmitted power is useful and the self-interference component is added to the Gaussian channel noise. Even if we were able to remove entirely the negative impact of the self-interference term in each frequency, we could not avoid a certain performance degradation, expressed by η_S, due to the useless transmitted power inherent to the self-interference component. Table I shows some values of η_S when $g_C(|s_n'|)$ corresponds to an ideal envelope clipping with normalized clipping level s_M/σ, for several clipping and filtering iterations.

For an iterative transmitter, the filtering effect inherent to the coefficients α_k^{Tx} eliminates the orthogonality between different spreading codes, even for an ideal additive white gaussian noise (AWGN) channel, leading to an additional degradation. The filtering effect could be compensated at the transmitter by multiplying S_k^{Tx} by $1/\alpha_k^{Tx}$. However, this produces an additional PMEPR regrowth of a few tenths of dB. As an alternative, we could restore the orthogonality between spreading codes through an appropriate chip-level equalization at the receiver. This is especially recommendable for CP-assisted DS-CDMA schemes employing FDE techniques [3], [4] since the equalizer can be designed for compensating both the filtering effects inherent to the coefficients α_k^{Tx} and the filtering effects associated to a time-dispersive channel. For an ideal AWGN channel and an FDE characterized by the multiplying coefficients $1/\alpha_k^{Tx}$, there is a performance degradation factor of

$$\eta_{MF} \approx \frac{1}{N^2} \sum_{k=0}^{N-1} E\left[|\alpha_k^{Tx}|^2\right] \sum_{k=0}^{N-1} E\left[|\alpha_k^{Tx}|^{-2}\right] \tag{26}$$

relatively to the case where α_k^{Tx} is constant. Since in our case α_k^{Tx} is almost constant, η_{MF} is very close to one. The receiver described in the following section performs this compensation together with the FDE procedure.

It is shown in Appendix A that the BER for an ideal AWGN channel is approximately given by

$$P_b \approx Q\left(\sqrt{SNR_{Tx,r'}}\right), \tag{27}$$

where the equivalent signal-to-noise ratio for the detection of the r'th spreading code is given by

$$SNR_{Tx,r'} = \frac{P_{Tx,r'}^S}{P_{Tx}^I + N_{eq}} = \frac{SIR_{Tx,r'}}{1 + N_{eq}/P_{Tx}^I}, \tag{28}$$

with $SIR_{Tx,r'} = \eta_{\xi,r'} SIR_{Tx}$ [see (58)], i.e., the codes with smaller power face stronger nonlinear distortion effects. This formula is very accurate as shown in Fig. 5, where $N = K = 256$ and a normalized clipping level of $s_M/\sigma = 0.5$.

V. RECEIVER DESIGN

A. Receiver Structure

Since the orthogonality between spreading codes is lost in a time-dispersive channel, we perform an FDE before the "despreading" procedure [4], [24]: after removing the CP, the received time-domain block $\{y_n; n = 0, 1, \ldots, N-1\}$ is passed to the frequency-domain by a DFT leading to the block $\{Y_k; k = 0, 1, \ldots, N-1\}$, where

$$Y_k = H_k S_k^{Tx} + N_k, \tag{29}$$

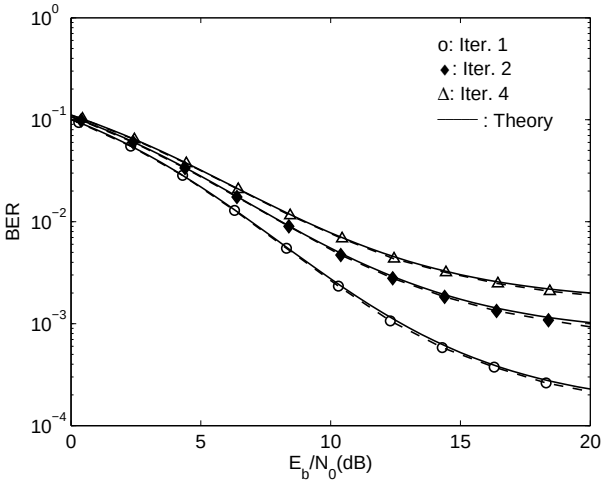

Fig. 5. Theoretical and simulation performance for an ideal AWGN channel for $N = K = 256$ and a normalized clipping level of $s_M/\sigma = 0.5$.

with H_k and N_k denoting the channel frequency response and the noise term for the kth frequency, respectively (as usually, it is assumed that the CP is longer than the overall channel impulse response).

Since $S_k^{Tx} = \alpha_k^{Tx} S_k + D_k^{Tx}$, it can be shown that the optimum FDE coefficients in the MMSE sense are given by

$$F_k = \frac{\alpha_k^{Tx*} E\left[|S_k|^2\right] H_k^*}{\left\{E\left[\left|\alpha_k^{Tx} S_k\right|^2\right] + E\left[\left|D_k^{Tx}\right|^2\right]\right\} |H_k|^2 + E\left[|N_k|^2\right]}, \quad (30)$$

where $E[|D_k^{Tx}|^2]$ can be obtained as described in Sec. III. The frequency-domain block at the output of the FDE is then $\{\tilde{S}_k; k = 0, 1, \ldots, N-1\}$, with

$$\tilde{S}_k = Y_k F_k. \quad (31)$$

The data block associated with the r'th spreading codes could be estimated by despreading the time-domain block at the FDE output, $\{\tilde{s}_n; n = 0, 1, \ldots, N-1\}$=IDFT$\{\tilde{S}_k; k = 0, 1, \ldots, N-1\}$, i.e., from the samples

$$\tilde{a}_{m,r'} = \sum_{n'=nK}^{nK+K} \tilde{s}_{n'} c_{n',r'}^*. \quad (32)$$

Clearly, the nonlinear effects lead to some BER degradation relatively to conventional DS-CDMA schemes, especially when a low PMEPR is intended and/or for codes with small assigned power. This degradation results from both the "useless" transmitted power spent on self-interference and the received self-interference being added to the channel noise.

To improve performance we consider the iterative receiver for CP-assisted multicode DS-CDMA depicted in Fig. 6. This receiver employs an IB-DFE with soft decisions [30], [31] (instead of the linear FDE) which is combined with estimation and compensation of nonlinear self-interference components. The receiver can be described as follows: For a given iteration, the signal at the output of the FDE is

$$\tilde{S}_k = F_k(Y_k - H_k \hat{D}_k^{Tx}) - B_k \overline{S}_k, \quad (33)$$

where $\{B_k; k = 0, 1, ..., N-1\}$ is the block of feedback coefficients, $\{\overline{S}_k; k = 0, 1, \ldots, N-1\}$ are the average values of $\{S_k; k = 0, 1, \ldots, N-1\}$ associated to the previous iteration, conditioned to the FDE output, and $\{\hat{D}_k^{Tx}; k = 0, 1, \ldots, N-1\}$ are estimates of the transmitted nonlinear self-interference components obtained by submitting $\overline{S}_k$ to a replica of nonlinear device at the transmitter (see Fig. 6) (it is assumed that the nonlinear characteristic $g_C(|s'_n|)$ adopted at the transmitter is known at the receiver). After the despreading operation, the data estimates for each spreading code $\{\overline{a}_{m,r'}\}$ are obtained by submitting $\{\tilde{a}_{m,r'}\}$ to a soft-decision device and used to form the estimates of the chip samples $\{\overline{s}_n; n = 0, 1, ..., N-1\}$.

We can also define a receiver that, as turbo equalizers, employs the channel decoder outputs instead of the uncoded soft decisions in the feedback loop of the IB-DFE. The receiver structure, that will be denoted as Turbo-FDE, is similar to the IB-DFE with soft decisions, but with soft-in-soft-out (SISO) channel decoder outputs employed in the feedback loop. The SISO block, that can be implemented as defined in [32], provides the log-likelihood ratios (LLR) of both the "information bits" and the "coded bits". The input of the SISO block are LLRs of the "coded bits" from the IB-DFE, after being appropriately deinterleaved[4].

B. Computation of Receiver Parameters

The optimum values of the feedforward and feedback coefficients, in the MMSE sense, are

$$F_k = \frac{\kappa \alpha_k^{Tx*} H_k^*}{\beta + \eta_k |H_k|^2 + (1-\rho^2)\left|\alpha_k^{Tx} H_k\right|^2} \quad (34)$$

and

$$B_k = F_k H_k \alpha_k^{Tx} - 1, \quad (35)$$

respectively, where κ is selected to ensure that $\sum_{k=0}^{N-1} F_k H_k \alpha_k^{Tx}/N = 1$,

$$\beta = \frac{E[|N_k|^2]}{E[|S_k|^2]}, \quad (36)$$

$$\eta_k = \frac{E\left[\left|D_k^{Tx} - \hat{D}_k^{Tx}\right|^2\right]}{E[|S_k|^2]}, \quad (37)$$

and the correlation coefficient ρ can be regarded as a measure of the reliability of the decisions used in the feedback loop, from the previous iteration, given by

$$\rho = \frac{\sum_{r=1}^{N_R} \xi_r^2 \sum_{r' \in \Psi_r} \rho_{r'}}{\sum_{r=1}^{N_R} \xi_r^2 K_r} \quad (38)$$

with

$$\rho_{r'} = \frac{K}{2N} \sum_{m=0}^{\frac{N}{K}-1} \left(|\text{Re}\{\overline{a}_{m,r'}\}| + |\text{Im}\{\overline{a}_{m,r'}\}|\right). \quad (39)$$

Note that, since $\rho = 0$ for the first iteration, the receiver reduces to a linear FDE optimized under the MMSE criterium [4]. After the first iteration, and if the residual BER is not too high (at least for the spreading codes for which a higher transmit power is associated), we have $\overline{a}_{m,r'} \approx a_{m,r'}$ for most of the data symbols, leading to $\overline{S}_k \approx S_k$. Consequently, we can use the feedback coefficients to eliminate a significant part of the residual interference.

It can be shown that the "overall chip averages" are

$$\overline{s}_n = \sum_{r=1}^{N_R} \xi_r \sum_{r' \in \Psi_r} c_{n,r'} \overline{a}_{\lfloor n/K \rfloor, r'}. \quad (40)$$

For a QPSK constellation, the average data values are

$$\overline{a}_{m,r'} = \tanh\left(\frac{\text{Re}\{\tilde{a}_{m,r'}\}}{\sigma_{r'}^2}\right) + \tanh\left(\frac{\text{Im}\{\tilde{a}_{m,r'}\}}{\sigma_{r'}^2}\right), \quad (41)$$

[4]As usual, it is assumed that the bits at the channel encoder output are interleaved before being mapped into the adopted constellation.

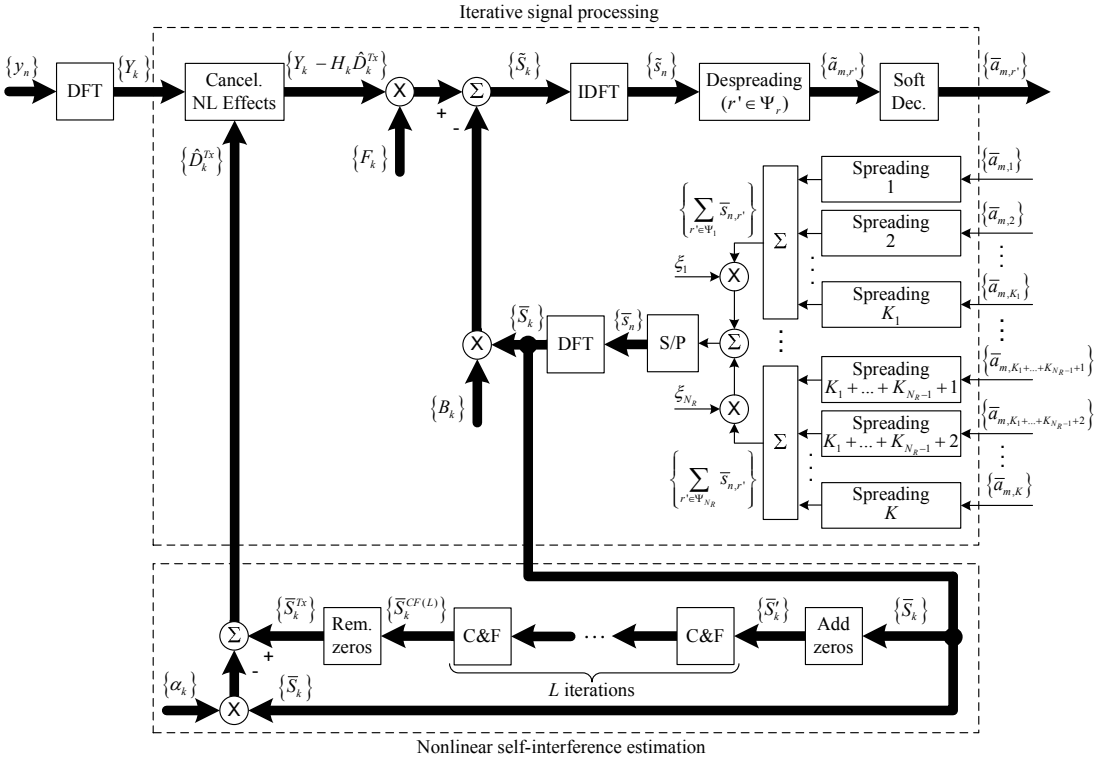

Fig. 6. Iterative receiver structure with estimation and compensation of nonlinear self-interference effects.

where $\tilde{a}_{m,r'}$ denotes the despreaded symbols and

$$\begin{aligned}\sigma^2_{r'} &= \frac{1}{2}E\left[\left|a_{m,r'} - \tilde{a}_{m,r'}\right|^2\right] \\ &\approx \frac{K}{2N}\sum_{m=0}^{\frac{N}{K}-1} E\left[\left|\hat{a}_{m,r'} - \tilde{a}_{m,r'}\right|^2\right], \end{aligned} \quad (42)$$

with $\hat{a}_{m,r'}$ denoting the hard decisions associated to $\tilde{a}_{m,r'}$.

With respect to η_k, for the first iteration $\hat{D}_k^{Tx} = 0$ and we can use the method of [13] to obtain $E[|D_k^{Tx}|^2|]$. For the remaining iterations it has to be obtained by simulation, as described in the following subsection.

C. Computation of Nonlinear Distortion Estimates

An important issue in our receiver is the estimation of nonlinear distortion effects. One possibility is to submit the soft-decision chip estimates $\{\overline{s}_n; n = 0, 1, ..., N-1\}$ to a replica of the nonlinear signal processing chain at the transmitter so as to obtain the self-interference estimates

$$\hat{D}_k^{Tx}\Big|_{\{\overline{s}_n\}} = \overline{S}_k^{Tx}\Big|_{\{\overline{s}_n\}} - \alpha_k^{Tx}\overline{S}_k, \quad (43)$$

where $\{\overline{S}_k; k = 0, 1, ..., N-1\}$ is the DFT of $\{\overline{s}_n; n = 0, 1, ..., N-1\}$ (as shown in Fig. 6).

As an alternative, we could also obtain the nonlinear distortion estimates by submitting the hard decisions $\{\hat{s}_n; n = 0, 1, \ldots, N-1\}$ to the nonlinear signal processing chain instead of $\{\overline{s}_n; n = 0, 1, \ldots, N-1\}$, i.e.,

$$\hat{D}_k^{Tx}\Big|_{\{\hat{s}_n\}} = \hat{S}_k^{Tx}\Big|_{\{\hat{s}_n\}} - \alpha_k^{Tx}\hat{S}_k, \quad (44)$$

where $\{\hat{S}_k; k = 0, 1, ..., N-1\}$ is the DFT of $\{\hat{s}_n; n = 0, 1, ..., N-1\}$. To avoid error propagation, these estimates could be weighted by the correlation coefficient ρ, which can be regarded as the overall reliability of the decisions used in the feedback loop. This leads to the estimates

$$\hat{D}_k^{Tx} = \rho\ \hat{D}_k^{Tx}\Big|_{\{\hat{s}_n\}}. \quad (45)$$

Fig. 7 shows the behavior of $E[|D_k^{Res}|^2]$, with $D_k^{Res} = D_k^{Tx} - \hat{D}_k^{Tx}$ denoting the residual nonlinear self-interference, as a function of ρ for the three estimates described above, for a normalized clipping level of $s_M/\sigma = 0.5$ (similar behavior was observed for other values of s_M/σ). From Fig. 7 we can observe that, for small values of ρ, using the estimates to remove nonlinear distortion effects can be worse than not doing it, i.e.,

$$E[|D_k^{Res}|^2] > E[|D_k^{Tx}|^2]. \quad (46)$$

Therefore, the compensation should only take place when the residual nonlinear self-interference is smaller than the nonlinear self-interference in the transmitted signals and when the reliability of the "overall chip" estimates is above a given threshold. From Fig. 7 it is also clear that the best estimates are the ones based on (45), which will be considered in the remaining of the paper. We will assume that

$$\begin{aligned} E\left[\left|D_k^{Res}\right|^2\right] &\approx f(\rho)E\left[|D_k^{Tx}|^2\right] \\ &= (a_1\rho^2 + a_2\rho + a_3)E\left[|D_k^{Tx}|^2\right], \end{aligned} \quad (47)$$

where a_1, a_2 and a_3 are coefficients that depend on the adopted normalized clipping level s_M/σ. The optimum values, obtained by simulation, are: $a_1 = -15.76$, $a_2 = 23.33$,

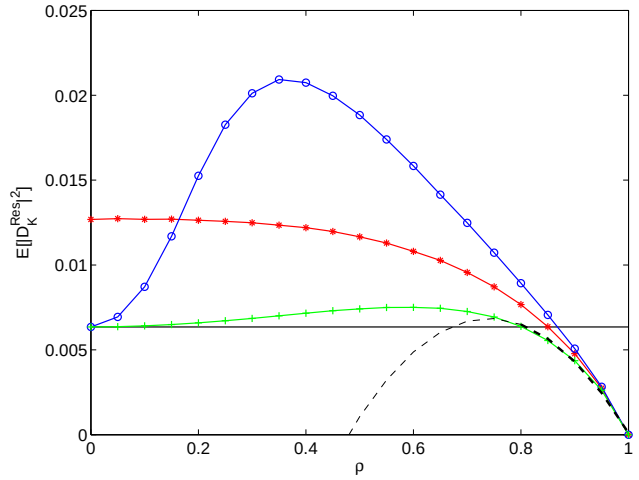

Fig. 7. $E[|D_k^{Res}|^2]$ as a function of ρ for a normalized clipping level of $s_M/\sigma = 0.5$: given by (43) (–o–); given by (44) (–∗–); given by (45) (–+–); true $E[|D_k|^2]$ (—) and given by approximation (47), with $a_1 = -15.76$, $a_2 = 23.33$ and $a_3 = -7.55$ (- - -).

$a_3 = -7.55$ for $s_M/\sigma = 0.5$; $a_1 = -11.36$, $a_2 = 15.92$, $a_3 = -4.56$ for $s_M/\sigma = 1.0$ and $a_1 = -9.48$, $a_2 = 12.70$, $a_3 = -3.21$ for $s_M/\sigma = 2.0$. Approximation (47), also included in Fig. 7, is used to compute η_k and as a threshold to trigger the compensation of nonlinear distortion effects (the compensation is performed when $f(\rho) \leq 1$ and $\rho > -a_2/(2a_1)$, i.e., the decreasing part of $f(\rho)$).

D. Implementation Issues

The implementation complexity of the proposed receiver can be measured in terms of the number and size of DFT/IDFT operations and the number of despreading/spreading operations. In the case of the IB-DFE receiver, we need one size-N DFT operation plus a pair of size-N IDFT/DFT operations and a pair of despreading/spreading operations at each iteration to detect a given resolution (except for the first iteration where only one size-N IDFT operation and a despreading operation are required). If we have estimation and compensation of nonlinear effects, L pairs of size-N IDFT/DFT operations for the detection of a given resolution at each iteration are also needed. In the case of the Turbo-DFE receiver, the SISO channel decoding needs to be implemented in the detection process, with the soft-input Viterbi algorithm instead of a conventional Viterbi algorithm.

It should be pointed out that our receiver can be simplified with only negligible performance degradation. This can be accomplished by noting that nonlinear distortion effects are mainly due to the spreading codes with higher assigned power. Therefore, in our multi-resolution scenario the lower resolutions (i.e., the ones with higher assigned power) are the ones that we should estimate with higher accuracy so as to obtain accurate estimates of nonlinear distortion effects. This means that if we are only able to detect up to a given resolution (e.g., due to our position relatively to the transmitter and/or due to hardware restrictions) we could ignore the resolutions which employ sets of spreading codes with lower assigned power[5]. Naturally, to detect the "higher" resolution (i.e., the resolution with the smaller assigned power) the receiver must detect all resolutions.

Another aspect that we could use to simplify the receiver is to note that if we have $\rho_r \approx 1$ for the rth resolution at a given iteration, this means that we already have reliable decisions for that resolution and we do not have to detect it again in the next iterations (in fact, we probably already have reliable decisions for all resolutions bellow r).

VI. Performance Results

In this section we present a set of performance results concerning our improved receivers for multi-resolution broadcasting in DS-CDMA systems employing CP-assisted block transmission techniques, combined with FDE schemes, where an iterative cancelation of deliberate nonlinear distortion effects is carried out. Unless otherwise stated, the transmitter (i.e., the BS) simultaneously transmits data blocks for $N_R = 4$ resolutions. The coded bits associated to each resolution are interleaved before being mapped into QPSK symbols under a Gray mapping rule (a bit-level random interleaving is performed over 5 fast Fourier transform (FFT) blocks). We consider an orthogonal spreading with $K_r = 64$, $r = 1, ..., 4$, spreading codes associated to each resolution and the same spreading factor $K = N = 256$ for all spreading codes (this corresponds to a fully loaded system). To reduce the PMEPR of the transmitted signals while maintaining the spectral occupations of conventional DS-CDMA signals, the BS performs an ideal envelope clipping operation, with normalized clipping level s_M/σ and an oversampling factor $M_{Tx} = N'/N = 2$, combined with a frequency-domain filtering operation, which can be jointly repeated several times. This procedure allows the PMEPR values and corresponding average SIR values shown in Table I (for conventional DS-CDMA schemes with a large number of spreading codes PMEPR$\approx$ 8.4 dB). The power amplifier at the transmitter is quasi-linear within the (reduced) range of variations of the input signal envelope. The receiver (i.e., the MT) knows the characteristic of the PMEPR-reducing signal processing technique employed by the transmitter. Perfect synchronization and channel estimation are assumed at the receiver.

We consider uncoded and coded BER performances with the well-known rate-1/2, 64-state convolutional code with generators $1+D^2+D^3+D^5+D^6$ and $1+D+D^2+D^3+D^6$. The SISO decoder is implemented using the Max-Log-MAP approach. As mentioned before, we will denote the receiver that employs uncoded soft decisions in the feedback loop as IB-DFE and the receiver with soft decisions from the SISO channel decoder outputs in the feedback loop as Turbo-FDE.

Let us first consider a case where all spreading codes have the same assigned power ($\xi_r = 1, r = 1, ..., 4$), corresponding to a single resolution transmission with a nonlinear transmitter with a normalized clipping level of $s_M/\sigma = 0.5$ and only one clipping and filtering (C&F) operation. Figs. 8 and 9 show the average BER performance for iterations 1 and 4 (naturally, the

[5]Moreover, the estimates for resolutions above the highest we are detecting will be very poor.

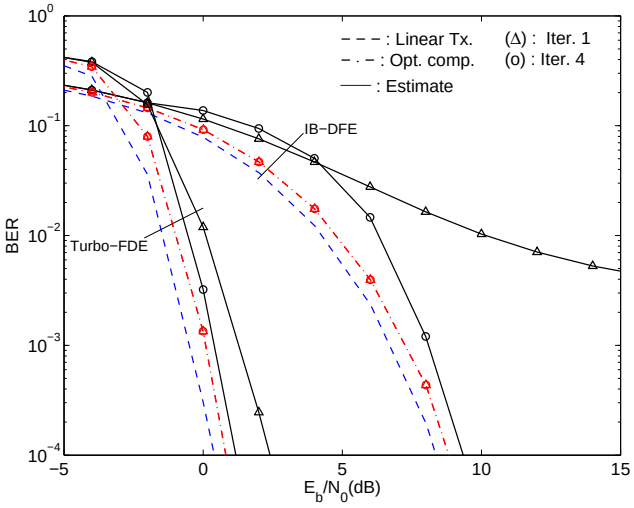

Fig. 8. Average BER performance for iterations 1 and 4 for an ideal AWGN channel, when $\xi_r = 1, r = 1, \ldots, 4$, for IB-DFE (uncoded BER) and Turbo-FDE (coded BER) receivers, when linear and nonlinear transmitters (optimum and estimated nonlinear distortion compensation) with normalized clipping level of $s_M/\sigma = 0.5$ are considered.

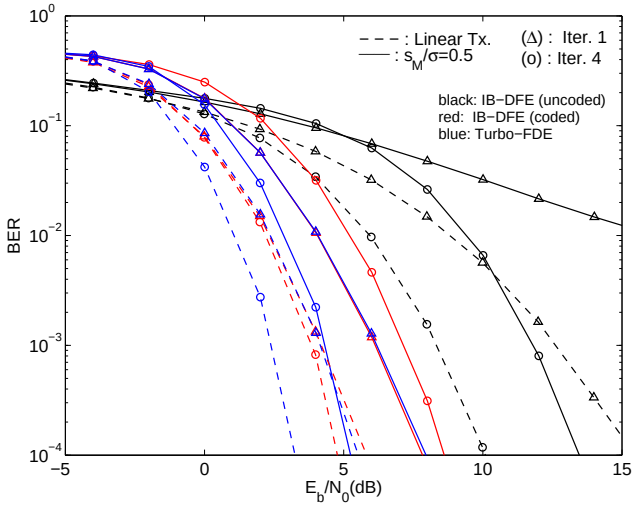

Fig. 9. As in Fig. 8, but for a severely time-dispersive channel.

first iteration corresponds to a linear receiver) for either IB-DFE and Turbo-FDE receivers. For the sake of comparisons, we also include the performance for a linear transmitter. Fig. 8 concerns an ideal Gaussian channel and Fig. 9 concerns a severely time-dispersive channel characterized by the power delay profile type C for the HIPERLAN/2 (HIgh PERformance Local Area Network) [33], with uncorrelated Rayleigh fading on the different paths. The duration of the CP is 1/5 of the duration of the useful part of the block (similar results were obtained for other severely time-dispersive channels). From Figs. 8 and 9 it is clear that the Turbo-FDE receiver allows good performance improvements relatively to the linear receiver for both channel types, which can be close to the one obtained with a linear transmitter. However, the uncoded BER performance of the IB-DFE receiver for the time-dispersive channel in Fig. 9, remains far from the linear transmitter performance, even after four iterations, and the coded BER performance trends to worse from iteration to iteration due to error propagation effects resulting from high nonlinear distortion effects.

Let us consider now a multi-resolution scenario with $\xi_1 = 1$, $\xi_2 = 1/2$, $\xi_3 = 1/4$ and $\xi_4 = 1/8$ (i.e., the power assigned to the rth resolution is 6 dB below the power assigned to the $(r-1)$th resolution), assuming again a nonlinear transmitter with $s_M/\sigma = 0.5$ and only one C&F operation. Figs. 10, 11 and 12 concern the same severely time-dispersive channel mentioned above and show, respectively, the uncoded and coded BER performance for the IB-DFE receiver, and the coded BER performance for the Turbo-FDE receiver, for iterations 1 and 4. We also include the performance for a linear transmitter. Clearly, the performance degradation due to the nonlinear distortion effects can be very high, especially for low-power resolutions. We can also observe that the Turbo-FDE receiver significantly outperforms the IB-DFE. As Fig. 13 shows, which concerns the coded BER performance for the Turbo-FDE receiver for the same multi-resolution scenario but with a not so low clipping level $s_M/\sigma = 1.0$, the performance trends to become closer to the one obtained with a linear transmitter.

Let us consider a case where we want a transmission with a very low-PMEPR of the DS-CDMA signals, not only by assuming a very low clipping level, but also by repeating several times the C&F operations to further reduce the PMEPR of the transmitted signals while maintaining the spectral occupation of conventional DS-CDMA schemes (see Table I). Fig. 14 shows the average coded BER performance for iterations 1 and 4 for Turbo-FDE receiver with 1, 2, 4 or 8 C&F iterations at the transmitter and a normalized clipping level of $s_M/\sigma = 0.5$. From this figure it is clear that the performance degradation associated to several clipping and filtering operations is relatively small when Turbo-FDE receivers with estimation and cancelation of nonlinear distortion effects are employed, in spite of the considerable PMEPR reduction of the transmitted signals.

VII. Conclusions and Final Remarks

In this paper we consider multi-resolution broadcasting in DS-CDMA systems employing clipping techniques combined with frequency-domain filtering, jointly performed in an iterative way, so as to reduce the envelope fluctuations and PMEPR of the transmitted signals, while maintaining the spectral occupation of conventional DS-CDMA signals.

We present an improved receiver design able to perform an iterative estimation and threshold-based cancelation of deliberate nonlinear distortion effects introduced at the transmitter. Our performance results show that we can improve significantly the performance with just a few iterations, even for severely time-dispersive channels and/or in the presence of strong nonlinear effects resulting when a very low-PMEPR of the transmitted signals is intended.

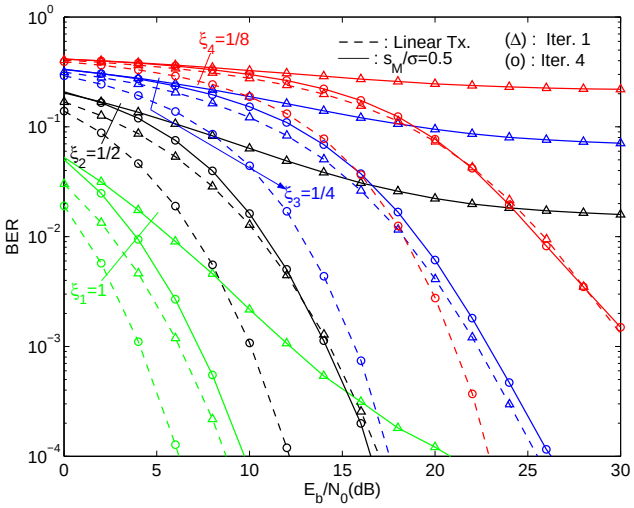

Fig. 10. Uncoded BER performance for iterations 1 and 4, when $\xi_1 = 1$, $\xi_2 = 1/2$, $\xi_3 = 1/4$ and $\xi_4 = 1/8$, for IB-DFE receiver, when linear and nonlinear transmitters with normalized clipping level of $s_M/\sigma = 0.5$ are considered.

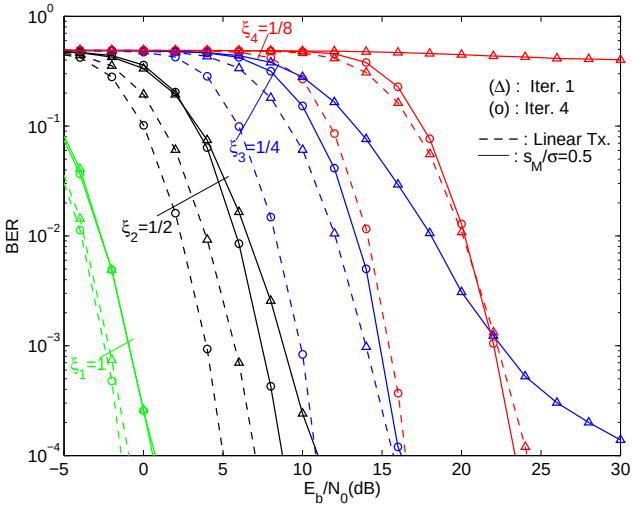

Fig. 11. Coded BER performance for the IB-DFE receiver, for the same scenario of Fig. 10.

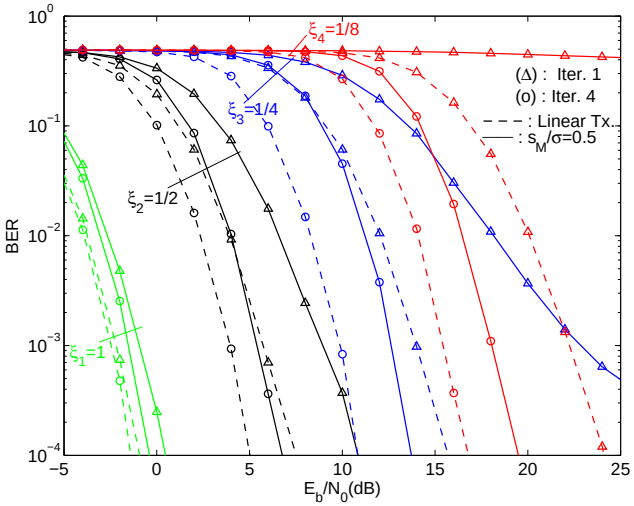

Fig. 12. As in Fig. 11, but for Turbo-FDE receiver.

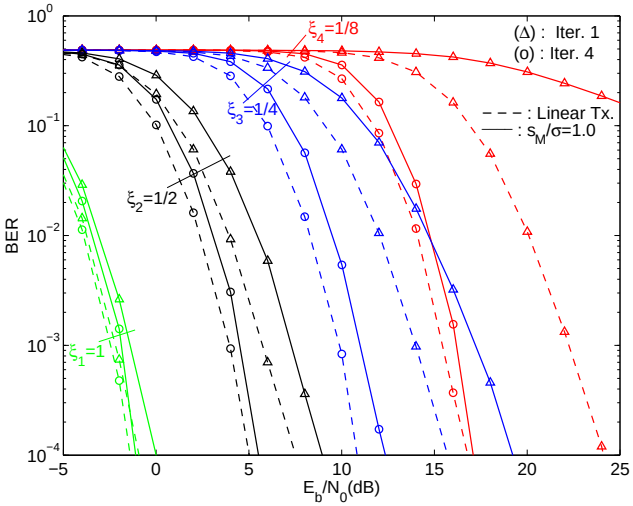

Fig. 13. As in Fig. 12, but with $s_M/\sigma = 1.0$.

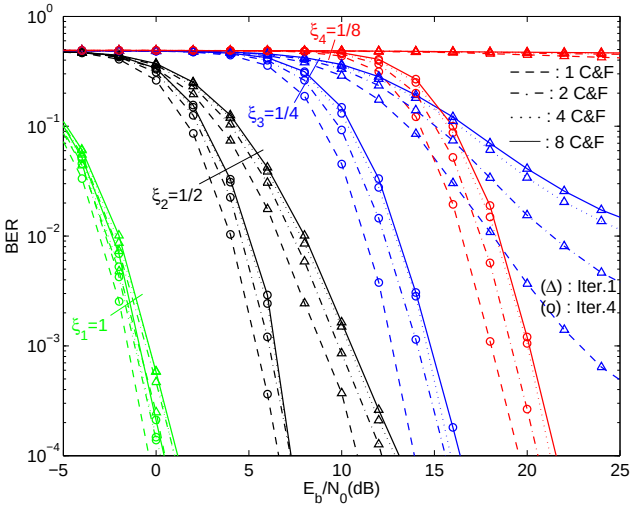

Fig. 14. Coded BER performance for iterations 1 and 4, when $\xi_1 = 1$, $\xi_2 = 1/2$, $\xi_3 = 1/4$ and $\xi_4 = 1/8$, for Turbo-FDE receiver, with 1, 2, 4 or 8 C&F iterations at the transmitter and a normalized clipping level of $s_M/\sigma = 0.5$.

APPENDIX

For an ideal Gaussian channel, the detection of the mth symbol transmitted by the r'th spreading code is based on

$$\tilde{a}_{m,r'} = \sum_{n=mK}^{mK+K-1} y_n c^*_{n,r'} = \sum_{n=mK}^{mK+K-1} s^U_n c^*_{n,r'} + d^{eq}_m + \nu^{eq}_m \quad (48)$$

$(m = 0, 1, ..., N/K - 1)$, where

$$y_n = s^{Tx}_n + \nu_n = s^U_n + d^{Tx}_n + \nu_n \quad (49)$$

denotes the output of the detection filter (assumed matched to the transmission filter $h_T(t)$) associated to the nth chip, with ν_n denoting the corresponding channel noise. In (48),

$$d^{eq}_m = \sum_{n=mK}^{mK+K-1} d^{Tx}_n c^*_{n,r'} \quad (50)$$

and

$$\nu_m^{eq} = \sum_{n=mK}^{mK+K-1} \nu_n c_{n,r'}^* \quad (51)$$

denote the equivalent self-interference and noise terms, respectively, for detection purposes.

Clearly, the power of the self-interference term, d_m^{eq}, is independent of m and given by

$$\begin{aligned} P_{Tx}^I &= \sum_{n=mK}^{mK+K-1} E\left[|d_n^{Tx}|^2\right] = \frac{K}{N}\sum_{n=0}^{N-1} E\left[|d_n^{Tx}|^2\right] \\ &= \frac{K}{N^2}\sum_{k=0}^{N-1} E\left[|D_k^{Tx}|^2\right] \end{aligned} \quad (52)$$

(it is assumed that $|c_{n,r'}| = 1$). The "useful" component for the detection of the mth symbol transmitted by the r'th spreading code is based on

$$\sum_{n=mK}^{mK+K-1} s_n^U c_{n,r'}^* \overset{(a)}{\approx} \overline{\alpha} \sum_{n=mK}^{mK+K-1} s_n c_{n,r'}^* \overset{(b)}{=} K\overline{\alpha} a_{m,r'}, \quad (53)$$

where $\{C_{k,r'}; k = 0, 1, \ldots, N-1\}$ is the DFT of $\{c_{n,r'}; n = 0, 1, \ldots, N-1\}$ and

$$\overline{\alpha} = \frac{1}{N}\sum_{k=0}^{N-1} \alpha_k^{Tx}. \quad (54)$$

In (53), (a) follows from $\alpha_k^{Tx} \approx \overline{\alpha}$ (see Fig. 4(a)) and (b) follows from the orthogonality of the spreading codes.

By assuming $E[|a_{m,r'}|^2] = 1$, the power of the "useful" component for the detection of the r'th spreading code of the rth resolution ($r' \in \Psi_r$) is

$$\begin{aligned} P_{Tx,r'}^S &\approx |K\overline{\alpha}|^2 = \frac{|K\overline{\alpha}\xi_r|^2 \sum_{n=0}^{N-1} E\left[|s_n|^2\right]}{N\sum_{r''=1}^{N_R} K_{r''}|\xi_{r''}|^2} \\ &= \frac{K|\overline{\alpha}\xi_r|^2}{N\overline{|\xi_r|^2}}\sum_{n=0}^{N-1} E\left[|s_n|^2\right] = \frac{K|\overline{\alpha}|^2\eta_{\xi,r}}{N}\sum_{n=0}^{N-1} E\left[|s_n|^2\right] \\ &= \frac{K|\overline{\alpha}|^2\eta_{\xi,r}}{N^2}\sum_{k=0}^{N-1} E\left[|S_k|^2\right] \overset{(a)}{\approx} \frac{K\eta_{\xi,r}}{N^2}\sum_{k=0}^{N-1} E\left[|\alpha_k^{Tx}S_k|^2\right], \end{aligned} \quad (55)$$

with (a) following, once again, from $\alpha_k^{Tx} \approx \overline{\alpha}$. In (55),

$$\overline{|\xi_r|^2} = \frac{1}{K}\sum_{r''=1}^{N_R} K_{r''}|\xi_{r''}|^2 \quad (56)$$

and

$$\eta_{\xi,r} = \frac{|\xi_r|^2}{\overline{|\xi_r|^2}}. \quad (57)$$

Therefore, the signal-to-self-interference ratio for the detection of the r'th spreading code is

$$SIR_{Tx,r'} = \frac{P_{Tx,r'}^S}{P_{Tx}^I} \approx \eta_{\xi,r'} SIR_{Tx}, \quad (58)$$

where the signal-to-self-interference ratio of the transmitted signal is given by

$$SIR_{Tx} = \frac{\sum_{n=mK}^{mK+K-1} E\left[|s_n^U|^2\right]}{\sum_{n=mK}^{mK+K-1} E\left[|d_n^{Tx}|^2\right]} = \frac{\sum_{k=0}^{N-1} E\left[|\alpha_k^{Tx}S_k|^2\right]}{\sum_{k=0}^{N-1} E\left[|D_k^{Tx}|^2\right]}. \quad (59)$$

When $K >> 1$, the term d_n^{eq} is approximately Gaussian-distributed. Therefore, if the data symbols are selected from a QPSK constellation under a Gray mapping rule (the extension to other constellations is straightforward) the BER for an ideal AWGN channel is approximately given by

$$P_b \approx Q\left(\sqrt{SNR_{Tx,r'}}\right), \quad (60)$$

where $Q(\cdot)$ denotes the well-known Gaussian error function and $SNR_{Tx,r'}$ denotes an equivalent signal-to-noise ratio for the detection of the r'th spreading code. This ratio is given by

$$SNR_{Tx,r'} = \frac{P_{Tx,r'}^S}{P_{Tx}^I + N_{eq}}, \quad (61)$$

with $N_{eq} = E[|\nu_n^{eq}|^2] = KE[|\nu_n|^2]$.

ACKNOWLEDGMENT

The authors would like to thank the reviewers for their helpful suggestions, based on which the quality of the paper has been improved.

REFERENCES

[1] A. Viterbi, *CDMA: Principles of SS Communication*, Addison Wesley, 1995.

[2] T. Ojamperä and R. Prasad, *Wideband CDMA for Third Generation Mobile Communications*, Artech House Publ., 1998.

[3] S. Barbarossa and F. Cerquetti, "Simple Space-Time Coded SS-CDMA Systems Capable of Perfect MUI/ISI Elimination", *IEEE Comm. Letters*, Vol. 5, No. 12, pp. 471–473, Dec. 2001.

[4] K. Baum, T. Thomas, F. Vook, V. Nangia, "Cyclic-Prefix CDMA: An Improved Transmission Method for Broadband DS-CDMA Cellular Systems", *IEEE WCNC*, Vol. 1, pp. 183–188, Orlando, USA, Mar. 2002.

[5] N. Guo and L. Milstein, "Uplink Performance Evaluation of Multicode DS/CDMA Systems in the Presence of Nonlinear Distortions", *IEEE J. on Sel. Areas in Comm.*, Vol. 18, No. 8, pp. 1418-1428, Aug. 2000.

[6] O. Väänänen, J. Vankka, T. Viero and K. Halonen, "Reducing the Crest Factor of a CDMA Downlink Signal by Adding Unused Channelization Codes", *IEEE Comm. Letters*, Vol. 6, No. 10, pp. 443–445, Oct. 2002.

[7] O. Väänänen, J. Vankka, T. Viero and K. Halonen, "Effect of Clipping in Wideband CDMA System and Simple Algorithm for Peak Windowing", *World Wireless Congress*, pp. 614–619. San Francisco, May, 2002.

[8] A. Palhau, R. Dinis, "Performance Evaluation of Signal Processing Schemes for Reducing the Envelope Fluctuations of CDMA Signals", *IEEE GLOBECOM'03*, Vol. 6, pp. 3392–3396, San Francisco, Dec. 2003.

[9] R. Dinis and A. Palhau, "A Class of Signal-Processing Schemes for Reducing the Envelope Fluctuations of CDMA Signals", *IEEE Trans. on Comm.*, Vol. 53, pp. 882–889, May 2005.

[10] R. Dinis and A. Gusmão, "A Class of Signal Processing Algorithms for Good Power Bandwidth Tradeoffs with OFDM Transmission", *IEEE ISIT'2000*, Sorrento, Italy, June 2000.

[11] J. Armstrong, "New OFDM Peak-to-Average Power Reduction Scheme", *IEEE VTC'2001 (Spring)*, Vol. 1, pp 756–760, Rhodes, Greece, May 2001.

[12] R. Dinis and A. Gusmão, "Performance Evaluation of an Iterative PMEPR-Reducing Technique for OFDM Transmission", *IEEE GLOBECOM'2003*, Vol. 1, pp. 20–24, Dec. 2003.

[13] R. Dinis and A. Palhau "A New Approach for Very Low-PMEPR Transmission in the Downlink of a DS/CDMA System", *IEEE VTC'04 (Spring)*, Milan, Italy, May 2004.

[14] R. Dinis and P. Silva, "An Iterative Detection Technique for DS-CDMA Signals with Strong Nonlinear Distortion Effects", *IEEE VTC'06 (Fall)*, pp. 1–5, Montreal, Canada, Sep. 2006.
[15] T. Cover, "Broadcast Channels", *IEEE Trans. on Inform. Theory*, Vol. 18, No. 1, pp. 2–14, Jan. 1972.
[16] K. Ramchandran, A. Ortega, K. Uz, and M. Vetterli, "Multiresolution Broadcast for Digital HDTV using Joint Source/Channel Coding", *IEEE J. Select. Areas Commun.*, Vol. 11, No. 1, pp. 6–23, Jan. 1993.
[17] J. Tellado, L. Hoo and J. Cioffi, "Maximum Likelihood Detection of Nonlinearly Distorted Multicarrier Symbols by Iterative Decoding", *IEEE Trans. on Comm.*, Vol. 51, No. 2, pp. 218–228, Feb. 2003.
[18] A. Gusmão and R. Dinis, "Iterative Receiver Techniques for Cancellation of Deliberate Nonlinear Distortion in OFDM-type Transmission", *Int. OFDM Workshop'04*, Dresden, Sep. 2004.
[19] A. Gusmão, R. Dinis and N. Esteves, "On Frequency-domain Equalization and Diversity Combining for Broadband Wireless Communications", *IEEE Trans. on Comm.*, Vol. 51, No. 7, pp. 1029–1033, July 2003.
[20] N. Benvenuto and S. Tomasin, "Block Iterative DFE for Single Carrier Modulation", *IEE Elec. Let.*, Vol. 39, No. 19, pp. 1144–1145, Sep. 2002.
[21] R. Dinis, A. Gusmão, and N. Esteves, "On Broadband Block Transmission over Strongly Frequency-Selective Fading Channels", *15th ICWC (Wireless 2003)*, pp. 261–269, Calgary, Canada, July 2003.
[22] R. Kalbasi, R. Dinis, D. Falconer and A. Banihashemi, "Layered Space-Time Receivers for Single-Carrier Transmission with Iterative Frequency-Domain Equalization", *IEEE VTC'04 (Spring)*, pp. 575–579, Milan, May 2004.
[23] R. Dinis, R. Kalbasi, D. Falconer and A. Banihashemi, "Iterative Layered Space-Time Receivers for Single-Carrier Transmission over Severe Time-Dispersive Channels", *IEEE Comm. Letters*, Vol. 8, No. 9, pp. 579–581, Sep. 2004.
[24] P. Silva and R. Dinis, "An Iterative Frequency-Domain Decision Feedback Receiver for CDMA Systems", *IEEE ISWCS'04*, pp. 6–10, Mauritius, Sep. 2004.
[25] R. Dinis, P. Silva and A. Gusmão, "IB-DFE Receivers with Space Diversity for CP-Assisted DS-CDMA and MC-CDMA Systems", *European Trans. on Telecomm.*, Vol. 18, No. 7, pp. 791-802, Nov. 2007.
[26] R. Dinis and A. Gusmão, "A Class of Nonlinear Signal Processing Schemes for Bandwidth-Efficient OFDM Transmission with Low Envelope Fluctuation", *IEEE Trans. on Comm.*, Vol. 52, No. 11, pp. 2009–2018, Nov. 2004.
[27] H. Rowe, "Memoryless Nonlinearities with Gaussian Input: Elementary Results", *Bell System Tech. Journal*, Vol. 61, Sep. 1982.
[28] G. Stette, "Caculation of Intermodulation From a Single Carrier Amplitude Characteristic", *IEEE Trans. on Comm.*, Vol. 22, No. 3, pp. 319–323, Mar. 1974.
[29] R. Dinis and A. Gusmão, "On the Performance Evaluation of OFDM Transmission Using Clipping Techniques", *IEEE VTC'99 (Fall)*, Vol. 5, pp. 2923–2928, Amsterdam, Sep. 1999.
[30] N. Benvenuto and S. Tomasin, "Iterative Design and Detection of a DFE in the Frequency Domain", *IEEE Trans. on Comm.*, Vol. 53, No. 11, pp. 1867–1875, Nov. 2005.
[31] A. Gusmão, P. Torres, R. Dinis and N. Esteves, "A Turbo FDE Technique for Reduced-CP SC-Based Block Transmission Systems", *IEEE Trans. on Comm.*, Vol. 55, No. 1, pp. 16-20, Jan. 2007.
[32] B. Vucetic and J. Yuan, *Turbo Codes: Principles and Applications*, Kluwer Academic Publ., 2002.
[33] ETSI, "Channel models for HIPERLAN/2 in Different Indoor Scenarios", *ETSI EP BRAN 3ERI085B*, pp. 1-8, March 1998.

Rui Dinis (S'96–M'00) received the Ph.D. degree from Instituto Superior Técnico (IST), Technical University of Lisbon, Portugal, in 2001. He was with IST from 2001 to 2008 and since 2008 he has been a Professor at Faculdade de Ciências e Tecnologia, Universidade Nova de Lisboa, Portugal. He was a member of the research center CAPS/IST (Centro de Análise e Processamento de Sinais), from 1992 to 2005, and a member of the research center ISR/IST (Instituto de Sistemas e Robótica), from 2005 to 2008. Since 2008 he has been a member of the Instituto de Telecomunicações (IT), Lisbon, Portugal. He has been involved in several research projects in the broadband wireless communications area. His main research interests include modulation, equalization and channel coding.

Paulo Silva received the M.Sc. degree from Instituto Superior Técnico (IST), Technical University of Lisbon, Portugal, in 1999. He is now preparing his Ph.D. thesis at IST. Since 1999 he has been a Professor with Instituto Superior de Engenharia (ISE), University of Algarve, Portugal. He was a member of the research center CAPS/IST (Centro de Análise e Processamento de Sinais), from 1995 to 2005, and a member of the research center ISR/IST (Instituto de Sistemas e Robótica), from 2005 to 2008. Since 2008 he has been a member of the Instituto de Telecomunicações (IT), Lisbon, Portugal. His main research interests concern spread spectrum techniques and multiuser detection.